
DOMAIN-AGNOSTIC AND MULTI-LEVEL EVALUATION OF GENERATIVE MODELS

Girmaw Abebe Tadesse
IBM Research - Africa
girmaw.abebe.tadesse@ibm.com

Jannis Born
IBM Research - Zurich
jab@zurich.ibm.com

Celia Cintas
IBM Research - Africa
celia.cintas@ibm.com

William Ogallo
IBM Research - Africa
william.ogallo@ibm.com

Dmitry Zubarev
IBM Research - Almaden
dmitry.zubarev@ibm.com

Matteo Manica
IBM Research - Zurich
tte@zurich.ibm.com

Komminist Weldemariam
IBM Research - Yorktown Heights
kommy@ibm.com

ABSTRACT

While the capabilities of generative models heavily improved in different domains (images, text, graphs, molecules, etc.), their evaluation metrics largely remain based on simplified quantities or manual inspection with limited practicality. To this end, we propose a framework for Multi-level Performance Evaluation of Generative mOdelS (MPEGO), which could be employed across different domains. MPEGO aims to quantify generation performance hierarchically, starting from a sub-feature-based low-level evaluation to a global features-based high-level evaluation. MPEGO offers great customizability as the employed features are entirely user-driven and can thus be highly domain/problem-specific while being arbitrarily complex (e.g., outcomes of experimental procedures). We validate MPEGO using multiple generative models across several datasets from the material discovery domain. An ablation study is conducted to study the plausibility of intermediate steps in MPEGO. Results demonstrate that MPEGO provides a flexible, user-driven, and multi-level evaluation framework, with practical insights on the generation quality. The framework, source code, and experiments will be available at: <https://github.com/GT4SD/mpego>.

Keywords Generative models · Evaluation · Data-centric AI · Foundation models

1 Introduction

Machine Learning (ML) methods, particularly generative models, are effective in addressing critical problems across different domains, which includes material sciences. Examples include the design of novel molecules by combining data-driven techniques and domain knowledge to efficiently search the space of all plausible molecules and generate new and valid ones [1, 2, 3, 4]. Traditional high-throughput wet-lab experiments, physics-based simulations, and bioinformatics tools for the molecular design process heavily depend on human expertise. These processes require significant resource expenditure to propose, synthesize and test new molecules, thereby limiting the exploration space [5, 6, 7].

For example, generative models have been applied to facilitate the material discovery process by employing inverse molecular design problem. This approach transforms the conventional and slow discovery process by mapping the desired set of properties to a set of structures. The generative process is then optimized to encourage the generation of molecules with those selected properties. Countless approaches have been suggested for such tasks, most prominently VAEs with different sampling techniques [8, 9, 10]), GANs [11, 12], diffusion models [13], flow networks [14] and Transformers [15].

Though the generation capability has been tremendously improved recently, the quantitative evaluation of these generative models in different domains remains a grand challenge [16]. Some of the reasons include the multi-objective nature of real discovery problems, the intricacy of evaluating relevant features *in-silico*, and the lack of widely accepted domain- and model-agnostic evaluation frameworks. As a result, existing benchmarks and toolkits in material sciences, such as MOSES [17] or GuacaMol [18] include limited metrics, such as validity and uniqueness, that lack the capacity to evaluate the complex nature of the generation process (e.g., interactions of multiple properties), thereby less effective to provide meaningful insights to subject matter experts (SMEs) to facilitate practical impact.

In this paper, we introduce a Multi-level Performance Evaluation of Generative mOdelS (MPEGO) framework (see Fig. 1), which aims to hierarchically characterize and quantify the capability of generative models, using material discovery domain as a use case. To that end, MPEGO is a model- and domain-agnostic framework, and its core design is derived from two main requirements: representative *examples* (of training and generated samples) and one or multiple *features* (extracted from these samples). Metrics derived from MPEGO are also interpretable and provide multi-level abstractions of the generation process. Specifically, the contributions of this paper are as follows:

1. We provide a multi-level and domain-agnostic evaluation of generative models, starting with sub-feature- or feature-based low-level evaluation to global features based high level-evaluation.
2. We devise a generation frequency analysis that aims to identify and characterize subsets of samples generated with extreme frequencies.
3. We validate MPEGO framework on multiple generative models (e.g., GCPN [19], GraphAF [20], MolGX [21] and Regression Transformer [15]), and multiple datasets (e.g., ZINC-250K [22] and MOSES [17] and CIRCA¹).
4. We conduct ablation studies to analyze MPEGO’s sensitivity to design choices.

2 Related Work

The state-of-the-art evaluation approaches for generative models aim to quantify pre-determined requirements, such as diversity and validity, using a variety of metrics. Frechet ChemNet Distance (FCD) [23] is one of such metrics, and it measures the distance between hidden representations drawn from sets of generated and training samples in the material discovery domain, which is limited in providing sub-feature or feature-level evaluation of models. GuacaMol [18] is one of the early benchmark platforms for new molecule discovery, which aims to evaluate generative models across different tasks, e.g., fidelity and novelty. Molecular Sets (MOSES) [17] is another benchmarking framework, which provides training and testing datasets, and a set of metrics to evaluate the quality and diversity of generated structures to standardize training and model comparisons.

Furthermore, automated characterization of subsets of samples, generated with more or less frequency, i.e., generation frequency analysis, also still remains challenging as the focus is more on latent- or feature-based evaluation. Overall, the challenges associated with evaluating generative models could be summarized as follows. First, multiple evaluation metrics are model-dependent. For example, FCD [23] depends on latent representation, and Maximum-mean discrepancy [24] is more specifically used to evaluate graph-based generative models. State-of-the-art metrics also suffer from limited generalizability (across different levels of feature interactions) and interpretability, e.g., by domain experts, which is critical to achieve trustworthy AI solutions [25]. In addition, existing evaluation metrics are susceptible to potential flaws in predictive models used in goal-oriented or constrained generation. Moreover, existing evaluation strategies lack a generic and standalone evaluation metric that combines both distributional metrics (e.g., uniqueness and diversity) and property-based metrics that score single property. The dependency on a single-constraint objective lacks a principled approach to incorporate multiple target features. This becomes a significant challenge when a single and inaccurate evaluation metric is used, which oversimplifies real discovery problems and hence less practical.

3 Proposed: MPEGO Framework

The proposed MPEGO framework (see Fig. 1) aims to provide an effective and multi-level characterization of generative models. The multi-level evaluation of MPEGO (see Fig. 2) starts from sub-feature-based low-level evaluation and their step-by-step aggregation to provide high-level evaluations. In this section, we first, formulate the critical research questions MPEGO framework is designed to address, followed by the details on its core components.

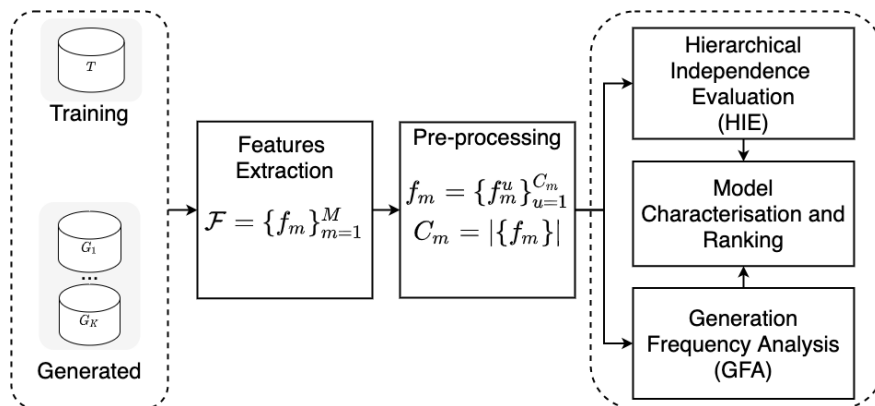


Figure 1: Overview of the MPEGO framework

3.1 Problem Statement

Let $\mathcal{G}_1, \mathcal{G}_2, \dots, \mathcal{G}_k, \dots, \mathcal{G}_K$ be datasets comprising samples generated from K black-box generative models $(\Theta_1, \Theta_2, \dots, \Theta_k, \dots, \Theta_K)$ trained on a dataset \mathcal{T} . Can we evaluate the generation capability of each Θ_i in a scalable, easily interpretable, and multi-objective manner? Specifically, we aim to address two questions.

- Q1: Given a set of features characterizing the samples, how do we quantify the generation capability of each model compared to another model or the training data, based on one or more of these features, i.e., at different levels of abstractions?
- Q2: What are the characteristics of samples being generated with extreme frequencies (least or most) by each of the generative models, compared with an other model or the training data, i.e., generation frequency analysis?

To address Q1, we propose a Hierarchical Independence Evaluation (HIE) that aims to quantify the performance of generative models at different levels of feature interactions hierarchically, starting with a sub-feature level evaluation (e.g., a specific range of a feature) to the global aggregation of multiple features. To address Q2, we employ multi-dimensional subset scanning (MDSS) [26] that aims to automatically identify and characterize over- and under-generated subsets of samples.

3.2 Feature Extraction and Pre-processing

Given representative examples of generated and training samples, MPEGO starts with the extraction of M features from these samples, $\mathcal{F} = \{f_1, f_2, \dots, f_m, \dots, f_M\}$. The type of feature values could be binary, continuous, or categorical, and a further pre-processing could be applied in the follow up steps. For example, discretization of continuous features is required for sub-feature-level performance evaluation, and MPEGO provides different discretization types, e.g., equal width, equal frequency or based on k -means.

3.3 Hierarchical Independence Evaluation (HIE)

HIE follows a bottom-up approach (from a sub-feature to global aggregation levels), as shown in Fig. 2, and it evaluates the performance generative models at different levels of feature interactions. The lowest level of evaluation in HIE is the sub-feature level independence score (SIS), which aims to quantify the performance of generative models across different ranges or unique values per feature, e.g., based on a molecular weight range of 200 – 300 Daltons. The second layer in HIE represents feature-level independence score (FIS), which quantifies the generation performance for each feature. To this end, FIS could be computed via aggregation of SIS values, thereby providing a weighting strategy for SIS scores per feature. FIS values could also be computed directly, without aggregating SIS values, using a different choice of objective measure is directly applied on the whole feature. The proposed MPEGO framework is flexible to utilize different objective measures (see Appendix D of the Supplementary Material for details). Below we describe the computation of SIS and FIS values, using Yule’s Y coefficient [27] as selected objective measure. Note that \mathcal{G}_k vs. \mathcal{T} refers to a case where the comparison is between the k th generative model and the training set \mathcal{T} . On the other hand, \mathcal{G}_k vs. \mathcal{G}_j refers to a case when the evaluation between the j th and k th models, where $j \neq k$. However, we stick with the \mathcal{G}_k vs. \mathcal{T} comparison below in order to ease readability.

¹<https://circa.res.ibm.com/>

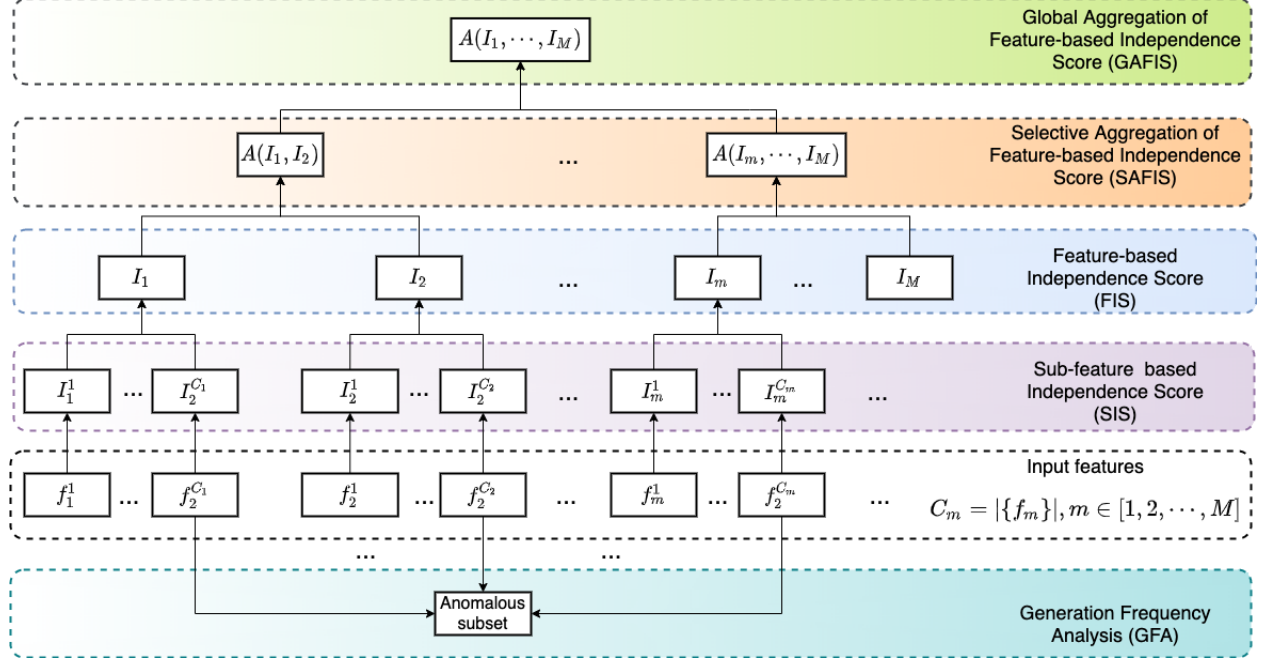


Figure 2: Details of Multi-level evaluation component of the MPEGO framework that comprises Hierarchical Independence Evaluation (i.e., SIS, FIS, SAFIS and GAFIS) and Generation Frequency Analysis (GFA). $A(\dots)$ represents aggregation operation, and anomalous subset refers to the logical combinations of features that characterize samples generated with extreme frequencies.

Let $f_m \in \mathcal{F}$ is a feature with C_m unique values or ranges, i.e., $f_m = \{f_m^u\}$, $u \in [1, 2, \dots, C_m]$. Note that C_m is the number of unique values for categorical features or the number of bins after discretization of continuous features. SIS computation requires the stratification of both the generated (\mathcal{G}_k) and training (\mathcal{T}) datasets per each unique value/range f_m^u resulting \mathcal{G}_{km}^u and \mathcal{T}_m^u , respectively. The complimentary subsets are then $\widetilde{\mathcal{G}}_{km}^u$ and $\widetilde{\mathcal{T}}_m^u$, respectively. Note that $\widetilde{\mathcal{G}}_{km}^u = \mathcal{G}_{km}^u | (f_m \neq f_m^u) = \mathcal{G}_k - \mathcal{G}_{km}^u$ and $\widetilde{\mathcal{T}}_m^u = \mathcal{T}_m^u | (f_m \neq f_m^u) = \mathcal{T} - \mathcal{T}_m^u$. Accordingly, a 2×2 pivot table is generated for each f_m^u as:

	$(f_m = f_m^u)$	$(f_m \neq f_m^u)$
\mathcal{G}_{km}	α	β
\mathcal{T}_m	δ	γ

where α is the number of generated samples in \mathcal{G}_{km}^u that are characterized by the feature value $f_m = f_m^u$, β is the number of generated samples in $\widetilde{\mathcal{G}}_{km}^u$ with $f_m \neq f_m^u$. Similarly, δ and γ are the numbers of training samples that satisfy $f_m = f_m^u$ in \mathcal{T}_m^u , respectively. Note that $\alpha + \beta$ are the total numbers of generated samples, i.e., $|\mathcal{G}_k|$. Similarly, $\delta + \gamma$ is the number of training samples, i.e., $|\mathcal{T}|$. Then Yule's Y coefficient is computed from the pivot table as $o_{km}^u \in [-1, 1]$:

$$o_{km}^u = \frac{\sqrt{P(\mathcal{G}_{km}^u)P(\widetilde{\mathcal{T}}_m^u)} - \sqrt{P(\widetilde{\mathcal{G}}_{km}^u)P(\mathcal{T}_m^u)}}{\sqrt{P(\mathcal{G}_{km}^u)P(\widetilde{\mathcal{T}}_m^u)} + \sqrt{P(\widetilde{\mathcal{G}}_{km}^u)P(\mathcal{T}_m^u)}} \quad (1)$$

$$o_{km}^u = \frac{\sqrt{\alpha\gamma} - \sqrt{\beta\delta}}{\sqrt{\alpha\gamma} + \sqrt{\beta\delta}} \quad (2)$$

SIS is then computed from o_{km}^u value as $I_{km}^u = 1 - |o_{km}^u|$, where $I_{km}^u \in [0, 1]$ and higher I_{km}^u reflects higher independence between \mathcal{G}_k and \mathcal{T} , i.e., SIS = 1 represents complete independence. Feature-level Independence Score (FIS), provides feature-based evaluation, i.e., higher abstraction than SIS. Depending on the objective measure, FIS could be computed as 1) via a weighted aggregation of SIS values, i.e., $I_{km} = \sum_{u=1}^{C_m} \lambda_{km}^u I_{km}^u$ where $\sum_{u=1}^{C_m} \lambda_{km}^u = 1$ and each λ_{km}^u weights the SIS value of f_m^u , or 2) via straightforward computation, without using SIS values, when

the objective measure is directly applied on each feature without discretization, e.g., using Wasserstein distance. The third layer of HIE is Selective Aggregation of Feature-level Independence Score (SAFIS), which aims to aggregate FIS values from $R < M$ selected features in \mathcal{F} . For example, features including scaffolding, fingerprints, aromaticity, and the number of rings could be selected to reflect the structural details of molecules in material discovery domain. The last layer of HIE is Global Aggregation of Feature-level Independence Score (GAFIS), which is computed via a weighted aggregation of all the FIS values in \mathcal{F} . Note that SAFIS and GAFIS are computed as $\hat{I} = \sum_{r=1}^R \eta_r I_{kr}$, where $\sum_{r=1}^R \eta_r = 1$, and $R < M$ for SAFIS and $R = M$ for GAFIS computation.

3.4 Generation Frequency Analysis (GFA)

Generative models trained on the same dataset will hardly generate samples with exact characteristics. Thus, there is a potential over- or under-generation of samples with certain characteristics. To this end, we employ automated stratification of samples using multi-dimensional subset scanning (MDSS) [26, 28] to identify subset of samples generated with divergent frequencies. Specifically, to identify samples generated with divergent rates by model Θ_k , compared to the training set \mathcal{T} , we first merge the corresponding datasets as $\mathcal{D} = \mathcal{G}_k \cup \mathcal{T}$, and an outcome label (y) is generated, such that $y_i = 1$ for a sample in \mathcal{G}_k and $y_i = 0$ for a sample in \mathcal{T} . If there are $N_g = |\mathcal{G}_k|$ generated and $N_t = |\mathcal{T}|$ training samples in \mathcal{D} , the expectation of generated samples in \mathcal{D} is $e_g = \frac{N_g}{N_g + N_t}$. Thus, GFA aims to identify a group of samples with extreme deviations in their generation rate compared to e_g . The deviation between the expectation and observation is evaluated by maximizing a Bernoulli likelihood ratio scoring statistic, $\Gamma(\cdot)$. The null hypothesis assumes that the odds of the generated sample in any subgroup \mathcal{S} is similar to the expected, i.e., $H_0 : odds(\mathcal{S}) = \frac{e_g}{1-e_g}$; while the alternative hypothesis assumes a constant multiplicative increase in the odds of the generated samples in \mathcal{S} , i.e., $H_1 : odds(\mathcal{S}) = q \frac{e_g}{1-e_g}$ where $q \neq 1$. Note that $q > 1$ for over-generated subset, and $0 < q < 1$ for under-generated subset. The divergence score for a subgroup (\mathcal{S}) with reference \mathcal{D} is formulated as, $\Gamma(\mathcal{S}, \mathcal{D})$ and computed as:

$$\Gamma(\mathcal{S}, \mathcal{D}) = \max_q \log(q) \sum_{i \in \mathcal{S}} y_i - N_s * \log(1 - e_g + qe_g), \quad (3)$$

where N_s is the number of samples in \mathcal{S} . The divergent subset, \mathcal{S} , identification is iterated until convergence to a local maximum is found, and the global maximum is subsequently optimized using multiple random restarts.

4 Experimental Setup

4.1 Training Datasets

We employed three different datasets in material discovery domain to validate our MPEGO framework.

ZINC-250K We utilize the publicly available ZINC-250K² dataset, which contains 249,455 small molecules in Simplified Molecular-Input Line-Entry System (SMILES) representation. Details on ZINC tool are available in [22].

MOSES The benchmark platform MOSES [17], besides implementing popular molecular generation models and metrics, MOSES contains a refined dataset from ZINC³. The dataset has approximately 2M molecules in total, filtered by certain parameters such as molecular weight ranges, and number of rotatable bonds, among others.

CIRCA We used IBM’s Chemical Information Resources for Cognitive Analytics (CIRCA) platform⁴ to construct a dataset of organic salts relevant to production of semiconductors via photolithography with chemical amplification. Finally, we were able to evaluate environmental and toxicological properties of 866 anions, that comprise the dataset used in this study. Steps conducted to obtain final version of the dataset could be found in Appendix A in the Supplementary Material.

4.2 Generative Models

We utilized multiple generative models for our validation. Particularly, Graph Convolutional Policy Network (GCPN) [19] and a Flow-based Autoregressive (GraphAF) [20] were trained separately on ZINC-250K and MOSES

²<https://www.kaggle.com/datasets/basu369victor/zinc250k>

³<https://zinc.docking.org/>

⁴<https://circa.res.ibm.com/>

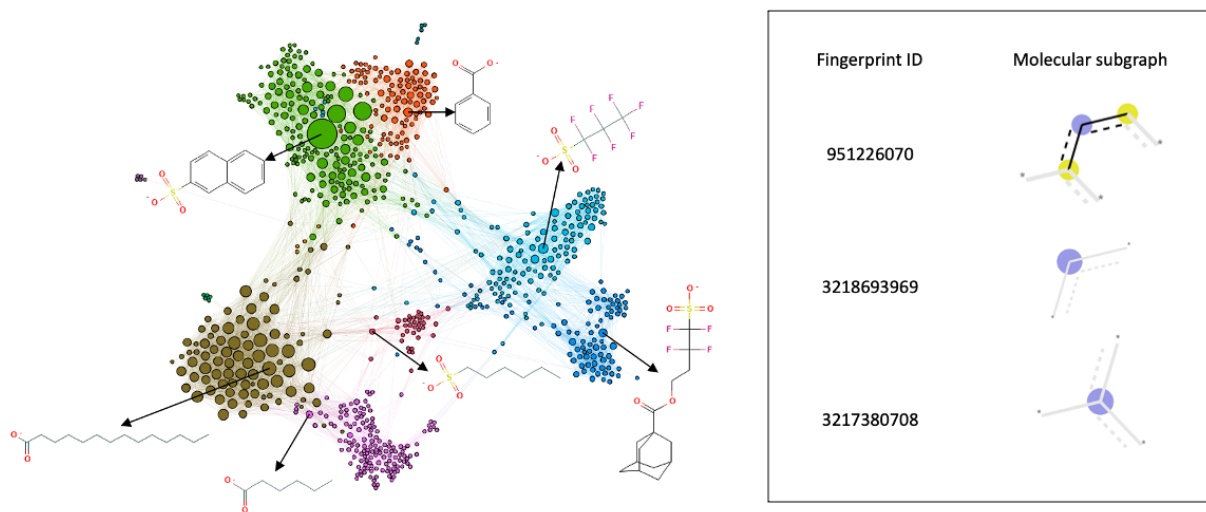


Figure 3: Visualization of the CIRCA dataset and some of the structural fingerprints relevant to MPEGO analysis (inset). The CIRCA dataset is represented as a similarity network, where nodes correspond to anions and links connect nodes if Dice similarity of the respective anions is at least 0.5. Node colors encode clustering recovered via modularity analysis and node size encodes the number of connections of the node. Chemical structures are included for the most connected nodes in the main clusters.

datasets. Subsequently, 10,000 valid molecules were generated from each model. We rely on GT4SD [29] for model implementations (experimental set-ups shown in Appendix B). Similarly, from the MOSES-trained GCPN and GraphAF, 14665 and 1680 molecules were generated respectively. For the CIRCA data, we employed MolGX [21] and the Regression Transformer [15]) and generated 5000 new anions with MolGX and 32617 new anions with Transformer. Note that balanced number of samples were selected across datasets during our experimentation, i.e., 10000, 1680 and 5000 samples were randomly selected for ZINC-250K-based, MOSES-based, CIRCA-based evaluations.

4.3 Feature Extraction and Preprocessing

We have extracted the following six features from SMILES representations of molecules in ZINC-250K and MOSES datasets and their corresponding generated datasets from GCPN and GraphAF. The following features are selected for the evaluation: *Aromaticity*, *ESOL*, *LogP*, *Weight*, *QED*, *SCScore*. On the other hand, we extracted fingerprints (see Fig. 3) that reflect structural details from CIRCA dataset and MolGX and Transformer generated datasets. Full details of features can be found in the Appendix C of the Supplementary Material. In cases when discretization of continuous features is required to compute the SIS values, we employ Yule’s Y coefficient as our default objective measure as it satisfies multiple key requirements [30]. We also employ equal frequency discretization type as it better handles outliers in the data, with five bins for ZINC and with three bins for CIRCA based evaluations. While aggregating features for SAFIS and GAFIS computations using normal averaging. Note that the proposed approach is flexible to utilize different discretization types, weighting strategies, and objective measures.

4.4 Evaluation Metrics

Our evaluation metrics include HIE’s SIS, FIS, SAFIS, and GAFIS values that quantify the generation independence of models. The independence score is obtained by normalizing the objective measure values to $[0, 1]$. Note independence score = 1.0 represents complete independence. We also utilize the histogram of features to provide a qualitative comparison. The characterization of generation frequency analysis involves using the logical combination of feature values to describe the identified subgroup, the size of the subgroup N_s , the odds ratio between \mathcal{S} and $\hat{\mathcal{S}} = \mathcal{D} - \mathcal{S}$, 95% Confidence Interval (CI) and empirical p value. We also reported the divergence score of the identified group from the expectation in GFA and elapsed time to identify the group. All the experiments are conducted on a desktop machine, 2.9 GHz Quad-Core Intel Core i7 (processor), and 16 GB 2133 MHz LPDDR3 (memory).

Table 1: HIE scores for GCPN and GraphAF models trained on ZINC-250K dataset

Level		\mathcal{G} vs. \mathcal{T}		\mathcal{G} vs. \mathcal{G}
		GCPN vs. ZINC	GraphAF vs. ZINC	GCPN vs. GraphAF
	Aromaticity	1.000	1.000	1.000
	ESOL	0.912	0.856	0.853
	LogP	0.951	0.942	0.906
FIS	Weight	0.656	0.713	0.809
	QED	0.946	0.666	0.662
	SCScore	0.825	0.752	0.866
SAFIS	QED+LogP	0.949	0.804	0.784
GAFIS		0.882	0.821	0.850

5 Results and Discussion

5.1 Hierarchical Independence Evaluation

Table 1 provides extended FIS values across each of the features considered for comparing GCPN and GraphAF models with the training ZINC-250K (\mathcal{G} vs. \mathcal{T}) and between each other - head-to-head (\mathcal{G} vs. \mathcal{G}). GCPN’s GAFIS value of 0.882, demonstrating competitive generation independence with GraphAF with GAFIS = 0.821. This is further shown with their head-to-head comparison, with Aromaticity ($FIS = 1.0$) and LogP ($FIS = 0.906$) features. Divergent characteristics are also demonstrated when the two models were evaluated based on QED, Weight and ESOL features, achieving FIS of 0.853, 0.809, and 0.662, respectively in their head-to-head comparison. SAFIS values are shown as an example of aggregation synthetic metrics, QED and LogP, where GCPN model achieves superiority compared to GraphAF. GAFIS values in the bottom row are derived from global aggregation of FIS values above. Overall, the results show the flexibility of the MPEGO framework to evaluate models across different levels of feature interactions and comparison baselines, i.e., training data or another generated datasets.

Furthermore, Fig. 4 demonstrates the benefits of sub-feature level evaluation (SIS) of GCPN and GraphAF models trained on ZINC-250K, using Molecular Weight as a feature example. Five ranges of the molecular weight in Fig. 4 (a) resulted from the discretization of the feature necessary for SIS evaluations. Similarly to Table 1, the comparison is performed between generative models and with the training dataset. Results demonstrate that GCPN and GraphAF generated molecules with similar weight characteristics but distinctively different at a few particular ranges, i.e., GCPN generated molecules similar to ZINC-250K with range [258.1, 308.39) whereas GraphAF showed better resemblance with ZINC-250K at ranges [201.63, 258.1) and ≥ 361.47 Daltons. Divergent sub-level generation characteristics is also encoded by lower \mathcal{G} vs. \mathcal{G} independence score at those ranges. The histogram plot in Fig. 4 (b) qualitatively compliments the insights from SIS values in Fig. 4 (a), where GraphAF is shown to generate more molecules with extreme weight values. Note that such sub-feature level insights in Fig. 4 are unique to our proposed framework as they are currently limited in the state-of-the-art of generative model evaluation.

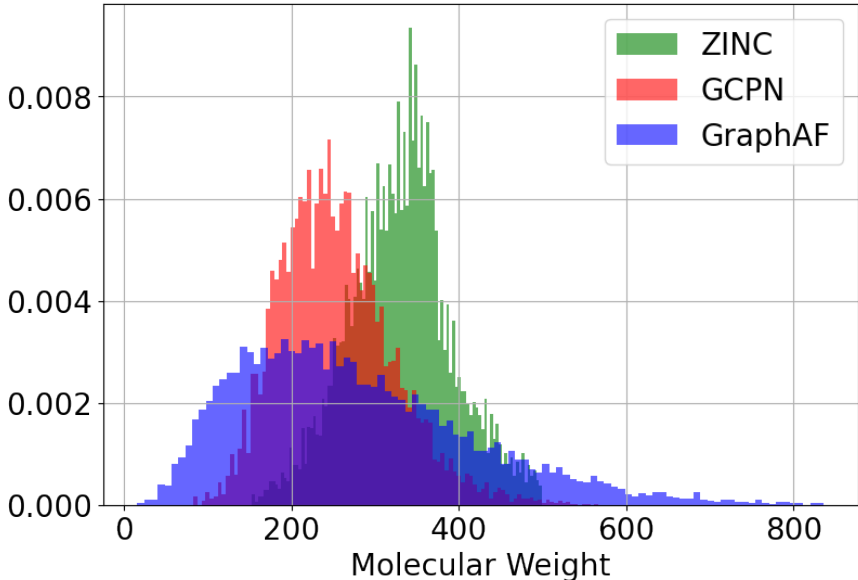
The results of comparisons of GCPN and GraphAF trained on MOSES dataset (Table 2) and MolGX and RT trained on CIRCA dataset (Table 3) demonstrate MPEGO’s capabilities further. Comparisons between Table 1 with Table 2 show while MOSES is used as a training, GraphAF achieved more independence than when ZINC-250K is used, compared GCPN. Between MolGX and the RT, trained on CIRCA, molecules generated from the RT achieved a higher resemblance with CIRCA than MolGX. In their head-to-head comparison, MolGX and RT generated mostly divergent structural details, as it is demonstrated by very low FIS values for the majority of the fingerprints in \mathcal{G} vs. \mathcal{G} column of Table 3.

5.2 Generation Frequency Analysis

Table 4 shows the divergence generation frequency of models, compared to the training or other generated set. For example, the GCPN model generated molecules with higher LogP (≥ 1.31) and lower weight (< 258.1 Daltons) compared to the training ZINC-250K. When we compare the two models head-to-head, GCPN tends to generate

Level	Weight Range	\mathcal{G} vs. \mathcal{T}		\mathcal{G} vs. \mathcal{G}
		GCPN vs. ZINC	GraphAF vs. ZINC	GCPN vs. GraphAF
SIS	<201.63	0.406	0.322	0.859
	[201.63 , 258.1)	0.631	0.840	0.778
	[258.1 , 308.39)	0.986	0.824	0.810
	[308.39 , 361.47)	0.671	0.637	0.962
	≥ 361.47	0.586	0.939	0.638

(a)



(b)

Figure 4: (a) Example of Molecular Weight-based SIS values that provide sub-feature level evaluation of GCPN and GraphAF models trained on ZINC-250K; (b) histogram densities to provide qualitative visualization of the SIS values in (a)

molecules with higher QED (≥ 0.64) values compared to GraphAF (< 0.5). When MOSES data is used as validation, LogP values become the differentiation factor as GraphAF tends to generate lower values (< 3.91) compared to GCPN (≥ 3.91). On CIRCA dataset, MolGX generates samples with a higher occurrence of '3217380708' fingerprint compared to the RT model and the training CIRCA. The size of the identified group, along with the multiplicative factor (q) and the odds ratio values, confirm the significance of the identified divergent generation in our generation frequency analysis.

5.3 Ablation Study

We conducted ablation studies to validate the robustness of MPEGO for different design choices of objective measures (see Fig. 5) and discretization types (see Fig. 6). Though objective measures could vary in whether they require discretization or not, the similar shapes of the plots in Fig. 5 demonstrate similar ranking performance across features. For example, in GCPN vs. ZINC comparison (Fig. 5 (a)), Molecular weight achieved the least score among features under all the different objective measures employed. The same is true for QED in the GraphAF vs. ZINC validation in Fig. 5 (b). We also validated the impact of the discretization types as shown in Fig.6 (a) and (b). In both cases, *equal width* and *k-means* discretizations provide similar patterns while *equal frequency* discretization demonstrated a slightly different pattern, particularly for features with skewed distribution as Aromaticity. Overall, all three types of discretization provide competitive performance scores, thereby validating the stability of our MPEGO framework. More ablation results are in Appendix E of the Supplementary Material.

Table 2: HIE Scores for GCPN and GraphAF models trained on MOSES dataset

Level		\mathcal{G} vs. \mathcal{T}		\mathcal{G} vs. \mathcal{G}
		GCPN vs. ZINC	GraphAF vs. ZINC	GCPN vs. GraphAF
	Aromaticity	1.000	1.000	1.000
	ESOL	0.419	0.672	0.491
	LogP	0.219	0.682	0.319
FIS	Weight	0.550	0.491	0.760
	QED	0.471	0.576	0.735
	SCScore	0.846	0.865	0.744
SAFIS	QED+LogP	0.345	0.629	0.527
GAFIS		0.584	0.714	0.675

Table 3: HIE Scores for MolGX and Regression Transformer (RT) models trained on CIRCA dataset

Level	Fingerprint	\mathcal{G} vs. \mathcal{T}		\mathcal{G} vs. \mathcal{G}
		MolGX vs. MOSES	Transformer vs. MOSES	MolGX vs. Transformer
	951226070	1.000	1.000	1.000
	3218693969	0.599	0.876	0.500
	2968968094	1.000	1.000	1.000
FIS	882399112	1.000	1.000	1.000
	2245384272	0.998	0.847	0.845
	2246703798	1.000	1.000	1.000
	3217380708	0.411	0.661	0.226
GAFIS		0.858	0.912	0.796

6 Conclusion and Future Work

We proposed MPEGO - a simple, generalizable, and model-agnostic evaluation framework of generative models validated for material discovery domain. MPEGO consists of two main performance evaluation blocks: Hierarchical Independence Evaluation (HIE) and Generation Frequency Analysis (GFA). HIE follows a bottom-up approach to quantify the generation performance of a model, starting from per sub-feature level (at the bottom) to the global aggregation of features (at the top). Thus, HIE provides a flexible performance evaluation of generative models. Particularly by evaluating the generation independence of models compared with the training data or other generative models using an objective measure set by a user. GFA is applied to detect and characterize divergent generation characteristics. Different from the existing evaluation platforms, MPEGO provides interpretable insights that aim to facilitate interactions with subject matter experts, which is crucial to develop Trustworthy AI solutions. The proposed MPEGO toolkit was validated with multiple datasets (ZINC-250K, MOSES, and CIRCA) and generative models trained on these datasets, including GCPN, GraphAF, MolGX, and RT. Conditioned on the training samples in these datasets, GCPN, GraphAF, and RT achieved higher generation independence, compared to their counterparts, GraphAF, GCPN, and MolGX models, respectively. Future work aims to evaluate generative models from different domains to further validate the domain-agnostic nature of the MPEGO framework. We also plan to utilize MPEGO to improve the efficiency of latent-based analyses, such as creativity characterization [31] and out-of-distribution detection [32]. MPEGO will be natively integrated into the GT4SD, the Generative Toolkit for Scientific Discovery [29] and the source code and experiments will be available at: <https://github.com/GT4SD/mpego>.

Table 4: Results from generation frequency analysis, validated across three datasets: ZINC250K (with GCPN and GraphAF models), MOSES (with GCPN and GraphAF models), and CIRCA (with MolGX and RT). We also compared the models headtohead. The q factor represents the multiplicative increase in the odds of the outcome in the identified group compared to the null hypothesis. Elapsed time is in seconds.

Model	Baseline	Expected	Subset	Group size	Observed	q factor	Odds ratio	95% CI	pvalue	Score	Elapsed
GCPN	ZINC	0.5	LogP \geq 1.31 & Weight < 258.1	5228	0.888	7.952	13.98	(12.75, 15.33)	0.0	1781.619	9.21
	GraphAF	0.5	SCScore < 3.54 & QED \geq 0.64 & Weight < 362.48	8040	0.797	3.923	9.14	(8.54, 9.77)	0.0	1493.252	10.99
GraphAF	ZINC	0.5	SCScore \geq 2.62 & QED < 0.64 & Weight < 258.1	4072	0.946	17.425	27.71	(24.11, 31.85)	0.0	1949.670	8.96
	GCPN	0.5	QED < 0.5	5135	0.878	7.164	12.22	(11.17, 13.37)	0.0	1647.798	7.73
GCPN	MOSES	0.5	QED < 0.5 & 2.36 \leq LogP < 3.91	1422	0.985	66.714	397.89	(253.9, 623.53)	0.0	870.290	4.00
	GraphAF	0.5	LogP \geq 3.91 & Weight < 298.32	1284	0.992	127.400	525.01	(279.16, 987.37)	0.0	825.489	3.43
GraphAF	MOSES	0.5	Weight < 250.38 & -4.75 \leq ESOL < -3.59	915	0.991	113.375	245.40	(121.72, 494.77)	0.0	584.349	4.21
	GCPN	0.5	LogP < 3.91 & ESOL < -4.75 OR ESOL \geq -3.59 & Weight < 250.38	1297	0.976	40.839	162.96	(112.31, 236.46)	0.0	744.637	3.33
RT	CIRCA	0.5	2245384272 \geq 1.0	603	0.561	1.275	1.85	(1.43, 2.39)	0.0	2.430	1.92
	MolGX	0.5	3217380708 < 4.0 & 3218693969 < 2.0	353	0.989	87.250	286.60	(105.19, 780.82)	0.0	218.783	2.27
MolGX	CIRCA	0.5	3217380708 \geq 4.0	484	0.804	4.095	14.94	(10.99, 20.31)	0.0	93.805	2.30
	RT	0.5	3217380708 \geq 4.0	416	0.935	14.407	61.39	(39.48, 95.47)	0.0	186.404	2.11

References

- [1] Albert P Bartók, Sandip De, Carl Poelking, Noam Bernstein, James R Kermode, Gábor Csányi, and Michele Ceriotti. Machine learning unifies the modeling of materials and molecules. *Science advances*, 3(12):e1701816, 2017.
- [2] O Anatole von Lilienfeld and Kieron Burke. Retrospective on a decade of machine learning for chemical discovery. *Nature communications*, 11(1):1–4, 2020.
- [3] Tiago Sousa, João Correia, Vítor Pereira, and Miguel Rocha. Generative deep learning for targeted compound design. *Journal of Chemical Information and Modeling*, 61(11):5343–5361, 2021.
- [4] Samuel C Hoffman, Vijil Chenthamarakshan, Kahini Wadhawan, Pin-Yu Chen, and Payel Das. Optimizing molecules using efficient queries from property evaluations. *Nature Machine Intelligence*, 4(1):21–31, 2022.
- [5] Matthew D Lloyd. High-throughput screening for the discovery of enzyme inhibitors. *Journal of Medicinal Chemistry*, 63(19):10742–10772, 2020.
- [6] Pavel G Polishchuk, Timur I Madzhidov, and Alexandre Varnek. Estimation of the size of drug-like chemical space based on gdb-17 data. *Journal of computer-aided molecular design*, 27(8):675–679, 2013.
- [7] Joseph A DiMasi, Henry G Grabowski, and Ronald W Hansen. Innovation in the pharmaceutical industry: new estimates of r&d costs. *Journal of health economics*, 47:20–33, 2016.
- [8] Vijil Chenthamarakshan, Payel Das, Samuel Hoffman, Hendrik Strobelt, Inkit Padhi, Kar Wai Lim, Benjamin Hoover, Matteo Manica, Jannis Born, Teodoro Laino, et al. Cogmol: target-specific and selective drug design for covid-19 using deep generative models. *Advances in Neural Information Processing Systems*, 33:4320–4332, 2020.
- [9] Jannis Born, Matteo Manica, Joris Cadow, Greta Markert, Nil Adell Mill, Modestas Filipavicius, Nikita Janakara-jan, Antonio Cardinale, Teodoro Laino, and María Rodríguez Martínez. Data-driven molecular design for discovery and synthesis of novel ligands: a case study on SARS-CoV-2. *Machine Learning: Science and Technology*, 2(2):025024, 2021.

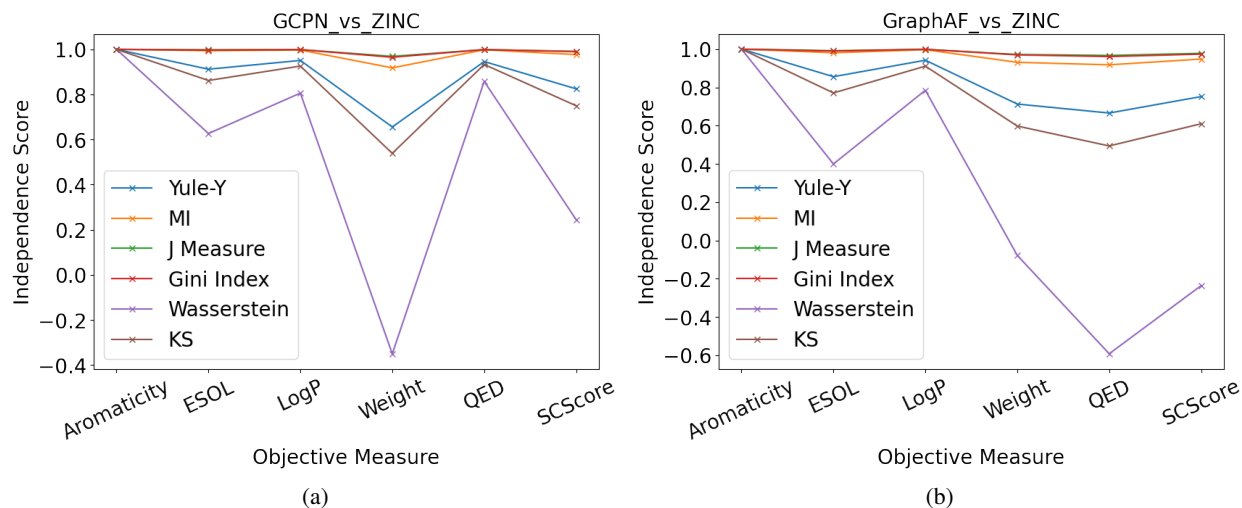


Figure 5: Different objective measures provided similar ranking per feature-level performance score (FIS) of the generative models

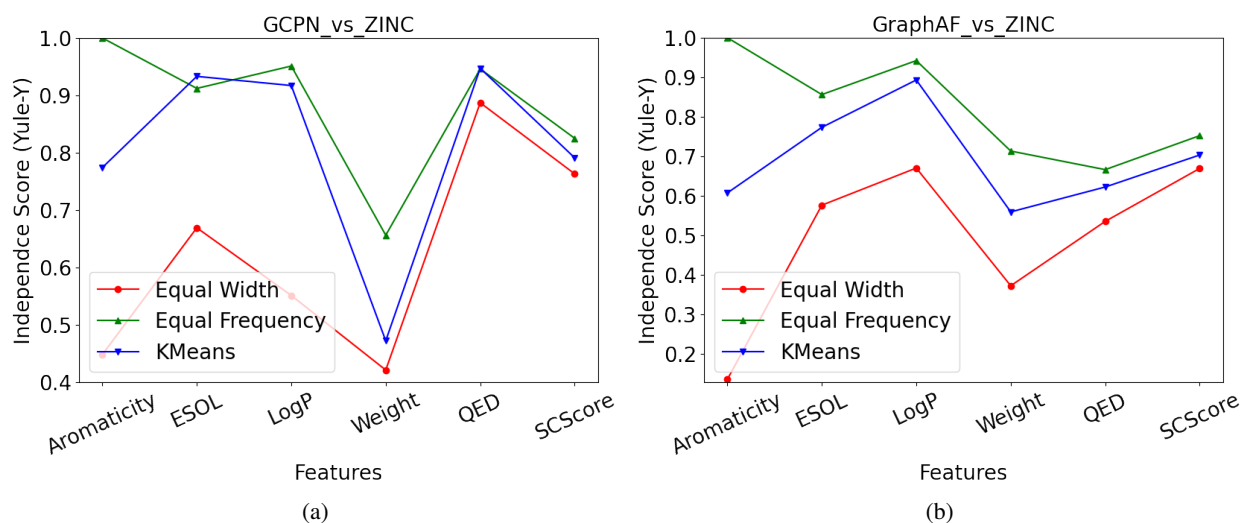


Figure 6: Different discretization types provided similar ranking per feature-level performance score (FIS) of the generative models

- [10] Jannis Born, Tien Huynh, Astrid Stroobants, Wendy D Cornell, and Matteo Manica. Active site sequence representations of human kinases outperform full sequence representations for affinity prediction and inhibitor generation: 3d effects in a 1d model. *Journal of Chemical Information and Modeling*, 62(2):240–257, 2021.
- [11] Oscar Méndez-Lucio, Benoit Baillif, Djork-Arné Clevert, David Rouquié, and Joerg Wichard. De novo generation of hit-like molecules from gene expression signatures using artificial intelligence. *Nature communications*, 11(1):1–10, 2020.
- [12] Łukasz Maziarka, Agnieszka Pocha, Jan Kaczmarczyk, Krzysztof Rataj, Tomasz Danel, and Michał Warchoła. Mol-cyclegan: a generative model for molecular optimization. *Journal of Cheminformatics*, 12(1):1–18, 2020.
- [13] Minkai Xu, Lantao Yu, Yang Song, Chence Shi, Stefano Ermon, and Jian Tang. Geodiff: A geometric diffusion model for molecular conformation generation. In *The Tenth International Conference on Learning Representations, ICLR, 2022*.
- [14] Moksh Jain, Emmanuel Bengio, Alex Hernandez-Garcia, Jarrid Rector-Brooks, Bonaventure FP Dossou, Chanakya Ajit Ekbote, Jie Fu, Tianyu Zhang, Michael Kilgour, Dinghui Zhang, et al. Biological sequence design

- with gflownets. In *International Conference on Machine Learning*, pages 9786–9801. PMLR, 2022.
- [15] Jannis Born and Matteo Manica. Regression transformer: Concurrent conditional generation and regression by blending numerical and textual tokens. *Nature Machine Intelligence*, 2023. In press.
- [16] Connor W Coley, Natalie S Eyke, and Klavs F Jensen. Autonomous discovery in the chemical sciences part ii: outlook. *Angewandte Chemie International Edition*, 59(52):23414–23436, 2020.
- [17] Daniil Polykovskiy, Alexander Zhebrak, Benjamin Sanchez-Lengeling, Sergey Golovanov, Oktai Tatanov, Stanislav Belyaev, Rauf Kurbanov, Aleksey Artamonov, Vladimir Aladinskiy, Mark Veselov, et al. Molecular sets (moses): a benchmarking platform for molecular generation models. *Frontiers in pharmacology*, 11:1931, 2020.
- [18] Nathan Brown, Marco Fiscato, Marwin HS Segler, and Alain C Vaucher. Guacamol: benchmarking models for de novo molecular design. *Journal of chemical information and modeling*, 59(3):1096–1108, 2019.
- [19] Jiaxuan You, Bowen Liu, Zhitao Ying, Vijay Pande, and Jure Leskovec. Graph convolutional policy network for goal-directed molecular graph generation. *Advances in neural information processing systems*, 31, 2018.
- [20] Chence Shi, Minkai Xu, Zhaocheng Zhu, Weinan Zhang, Ming Zhang, and Jian Tang. Graphaf: a flow-based autoregressive model for molecular graph generation. *arXiv preprint arXiv:2001.09382*, 2020.
- [21] Seiji Takeda, Toshiyuki Hama, Hsiang-Han Hsu, Victoria A Piunova, Dmitry Zubarev, Daniel P Sanders, Jed W Pitera, Makoto Kogoh, Takumi Hongo, Yenwei Cheng, et al. Molecular inverse-design platform for material industries. In *Proceedings of the 26th ACM SIGKDD International Conference on Knowledge Discovery & Data Mining*, pages 2961–2969, 2020.
- [22] John J Irwin, Teague Sterling, Michael M Mysinger, Erin S Bolstad, and Ryan G Coleman. Zinc: a free tool to discover chemistry for biology. *Journal of chemical information and modeling*, 52(7):1757–1768, 2012.
- [23] Kristina Preuer, Philipp Renz, Thomas Unterthiner, Sepp Hochreiter, and Gunter Klambauer. Frechet chemnet distance: a metric for generative models for molecules in drug discovery. *Journal of chemical information and modeling*, 58(9):1736–1741, 2018.
- [24] Arthur Gretton, Karsten M Borgwardt, Malte J Rasch, Bernhard Schölkopf, and Alexander Smola. A kernel two-sample test. *The Journal of Machine Learning Research*, 13(1):723–773, 2012.
- [25] Weixin Liang, Girmaw Abebe Tadesse, Daniel Ho, L Fei-Fei, Matei Zaharia, Ce Zhang, and James Zou. Advances, challenges and opportunities in creating data for trustworthy ai. *Nature Machine Intelligence*, 4(8):669–677, 2022.
- [26] Daniel B Neill, Edward McFowland III, and Huanian Zheng. Fast subset scan for multivariate event detection. *Statistics in Medicine*, 32(13):2185–2208, 2013.
- [27] G Udny Yule. On the methods of measuring association between two attributes. *Journal of the Royal Statistical Society*, 75(6):579–652, 1912.
- [28] Girmaw Abebe Tadesse, William Ogallo, Celia Cintas, and Skyler Speakman. Model-free feature selection to facilitate automatic discovery of divergent subgroups in tabular data. *arXiv preprint arXiv:2203.04386*, 2022.
- [29] Matteo Manica, Joris Cadow, Dimitrios Christofidellis, Ashish Dave, Jannis Born, Dean Clarke, Yves Gaetan Nana Teukam, Samuel C Hoffman, Matthew Buchan, Vijil Chenthamarakshan, et al. Gt4sd: Generative toolkit for scientific discovery. *arXiv preprint arXiv:2207.03928*, 2022.
- [30] Pang-Ning Tan, Vipin Kumar, and Jaideep Srivastava. Selecting the right objective measure for association analysis. *Information Systems*, 29(4):293–313, 2004.
- [31] Celia Cintas, Payel Das, Brian Quanz, Girmaw Abebe Tadesse, Skyler Speakman, and Pin-Yu Chen. Towards creativity characterization of generative models via group-based subset scanning. *arXiv preprint arXiv:2203.00523*, 2022.
- [32] Hannah Kim, Girmaw Abebe Tadesse, Celia Cintas, Skyler Speakman, and Kush Varshney. Out-of-distribution detection in dermatology using input perturbation and subset scanning. In *2022 IEEE 19th International Symposium on Biomedical Imaging (ISBI)*, pages 1–4, 2022.

Appendix A: Steps to prepare CIRCA dataset

Initially, we carried out a patent search in CIRCA for ionic photoacid generators (PAGs) that are sulfonium or iodonium salts. We extracted anionic components of the sulfonium and iodonium salts, finding 493 unique anions. We ran additional CIRCA search to enrich the dataset with anions relevant to photolithography using the following query: "PAG" OR "photo-acid generator" OR "photo initiator" OR "acid generating agent" OR "photocationic initiator" OR "photocationic polymerization initiator" OR "cationic initiator" OR "cationic type initiator" The additional search returned ionic compounds with 1398 anions, 189 of these 1398 anions were among the initial 493 anions. We processed the set of collected anions, keeping only anions with charge -1 and more than 1 carbon atom, reducing the dataset to 1086 anions. Out of 1086 anions, we were able to evaluate environmental and toxicological properties of 866 anions, that comprise the dataset used in this study

Appendix B: Experimental Setup for GCPN and GraphAF training

Table 5: Summary of hyper-parameters set-up to train the two graph-based models: GCPN and GraphAF using ZINC-250K dataset.

Setting	Models	
	GCPN	GraphAF
Input Dimension	18	9
Number of relation	3	3
Batch normalization	False	True
Atom types	[6-9, 15-17, 35, 53]	[6-9, 15-17, 35, 53]
Hidden dimensions	[256, 256, 256, 256]	[256, 256, 256]

Appendix C: Descriptions of features

Table 6: Features extracted from samples generated from GCPN and GraphAF models trained on ZINC-250k and MOSES datasets.

Feature	Description
QED	Qualitative Estimate of Drug-likeness
ESOL	Estimated SOLubility
SCScore	Synthetic Complexity Score
SAS	Synthetic Accessibility Score.
Scaffold	A molecule is identical to its scaffold
Ring	A molecule contains a ring structure
LargeRing	A molecule contains a ring structure with more than 6 atoms
Aromatic	A molecule contains an aromatic ring
StereoCharacter	SMILES string contains a stereochemistry string.
Stereocenter	Whether a molecule contains a stereocenter,
Heterocycle	A molecule has at least one ring with at least two different atoms
Lipinski	A molecule adheres to the Lipinski’s rule of five.
HBondDonor	A molecule has not more than 5 hydrogen bond donors
HBondAcceptor	A molecule has not more than 10 hydrogen bond acceptors
MolecularWeight	The molecular mass in Daltons
LogP	Logarithmic partition coefficient

Multiple fingerprints, informing the presence of particular structural elements in a given molecule, are extracted from CIRCA dataset and samples generated from MolGX and RT models. The following fingerprints are selected for evaluation in this study due to their higher variance across the datasets.






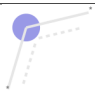

Fingerprint	Molecular Subgraph
2245384272	
951226070	
3217380708	
2246703798	
882399112	
3218693969	
2968968094	

Table 7: Fingerprints (and their molecular subgraph visualizations) selected for evaluations in CIRCA datasets and its associated models: MolGX and RT.

Appendix D: List of Objective measures

The MPEGO framework could handle different objective measures to quantify sub-feature or feature-level-based association between generated and training datasets or between two generated datasets. The list of objective measures implemented in the MPEGO framework includes: *Odds ratio*, *Yule's Y Coefficients*, *Yule's Q coefficients*, *Mutual Information*, *J Measure*, *Gini Index*, *Wasserstein Distance*, *Kstest*, *Support*, *Confidence*, *Laplace*, *Collective Strength*, *Kappa*, *Conviction*, *Interest*, *Cosine*, *Piatetsky Shapiro*, *Certainty Factor*, *Added Value*, *Jaccard* and *Kolmogorov–Smirnov*.

Appendix E: Ablation results

Similar ablation studies are applied for head-to-head comparison of models as shown in Fig. 7, where the robustness of the MPEGO framework is demonstrated across varieties of objective measures (Fig. 7 (a)) and discretization types (Fig. 7 (b)).

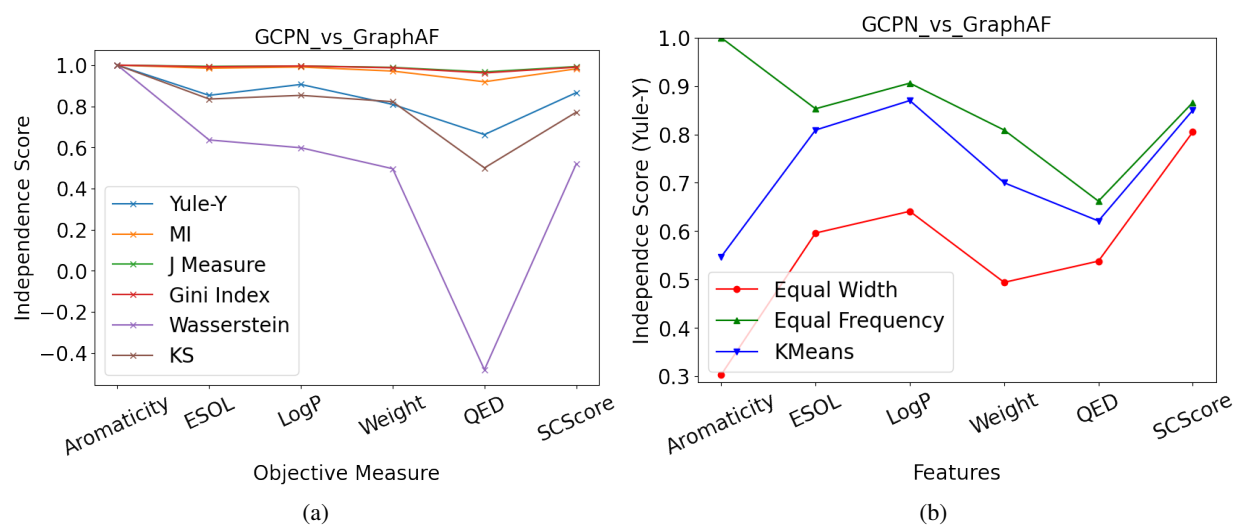


Figure 7: Results from the ablation study on the variations of (a) objective measures and (b) discretization types on the FIS values, validated with a head-to-head comparison of GCPN and GraphAF models, trained on ZINC-250K.